The Dynamical Origin of $m_{\phi,\mathrm{crit}} \simeq 1.965$: Phase-Boundary Physics in Siamese Universes

CosmicThinker[1] and ChatGPT (Toko)[2]

[1]Independent Researcher
[2]AI Research Assistant

November 17, 2025

Abstract

In the Phase–Bifurcation Cosmogenesis scenario, the early universe is described by a CPT–symmetric pair of "Siamese" branches that share a quantum vacuum at a bifurcation surface and then acquire a relative phase difference $\Delta\phi$ as they evolve. The late-time fate partitions into three sectors: (A) synchrony ($\Delta\phi \to 0$), (B) antipodal (trapping near π), and (C) escape/oscillatory (recurrent barrier crossing). A sharp transition in the synchrony probability P_A at an effective phase mass $m_{\phi,\mathrm{crit}} \simeq 1.965$ was reported previously. We reanalyse its origin and robustness with a controlled grid scan over $(m_\phi, k_{\mathrm{rot}})$, using $N_\Delta = 40$ initial phases per grid point and uniform sampling in $\Delta\phi_{\mathrm{ini}} \in [0, \pi)$. We confirm a clean monotonic transition in $P_A(m_\phi)$ with a global $m_{\phi,\mathrm{crit}}$ and find that the probability band in $(m_\phi, k_{\mathrm{rot}})$ is nearly vertical: m_ϕ is the primary control parameter, while k_{rot} produces a modest modulation peaking around $k_{\mathrm{rot}} \simeq 0.33$. Phase portraits at $m_{\phi,\mathrm{crit}}$ show a single stable spiral at $\Delta\phi = 0$ and a smooth separatrix. These results establish $m_{\phi,\mathrm{crit}}$ as a robust dynamical scale with implications for CPT-symmetric cosmology, baryogenesis and directional observables.

1 Introduction

CPT-symmetric cosmologies posit that our visible universe is mirrored by a partner evolving with the opposite arrow of time across the Big Bang [1–4]. In Siamese frameworks the relative phase between the branches becomes a physical degree of freedom. The phase mass m_ϕ controls whether the system locks in synchrony (A), is trapped antipodally (B), or escapes into oscillations (C), akin to driven-damped nonlinear oscillators [5–7]. Clarifying whether the previously reported value $m_{\phi,\mathrm{crit}} \simeq 1.965$ is a numerical artefact or a structurally stable feature is essential because P_A feeds directly into phase-locked vs. misaligned cosmological histories and thereby into baryogenesis pathways and large-scale anisotropies.

2 Effective phase dynamics

We treat $\Delta\phi$ as an angular variable with periodic potential

$$V_{\mathrm{eff}}(\Delta\phi) = m_\phi^2 \left[1 - \cos(\Delta\phi)\right], \tag{1}$$

leading, in $N = \ln a$, to

$$\Delta\phi'' + (3 + \xi(N))\,\Delta\phi' + m_\phi^2 \sin\Delta\phi = S_{\mathrm{rot}}(N; k_{\mathrm{rot}}), \tag{2}$$

with a decaying rotational source $S_{\mathrm{rot}}(N; k_{\mathrm{rot}}) = k_{\mathrm{rot}}\, e^{-\gamma N} f(N)$, $\gamma \simeq 2$. Initial conditions at N_{ini} adopt $\Delta\phi'(N_{\mathrm{ini}}) = 0$ and $\Delta\phi_{\mathrm{ini}} \in [0, \pi)$ uniformly.

3 Numerical setup and sector classification

We scan a 7×7 grid

$$m_\phi \in \{0.375,\, 0.75,\, 1.25,\, 1.625,\, 1.95,\, 2.5,\, 3.0\}, \tag{3}$$

$$k_{\rm rot} \in \{0.0,\, 0.083,\, 0.167,\, 0.25,\, 0.333,\, 0.417,\, 0.5\}, \tag{4}$$

and draw $N_\Delta = 40$ values of $\Delta\phi_{\rm ini}$ per point. Late-time, sector labels use time-averaged thresholds over $[N_f - \Delta N, N_f]$ with $\epsilon_\phi = 0.1$, $\epsilon_\pi = 0.1$, $\epsilon_{\phi'} = 0.05$.

4 Results

Global $P_A(m_\phi)$ and $m_{\phi,\rm crit}$.

$P_A(m_\phi, k_{\rm rot})$ and local $m_{\phi,\rm crit}(k_{\rm rot})$.

Phase-sector geometry and trajectories.

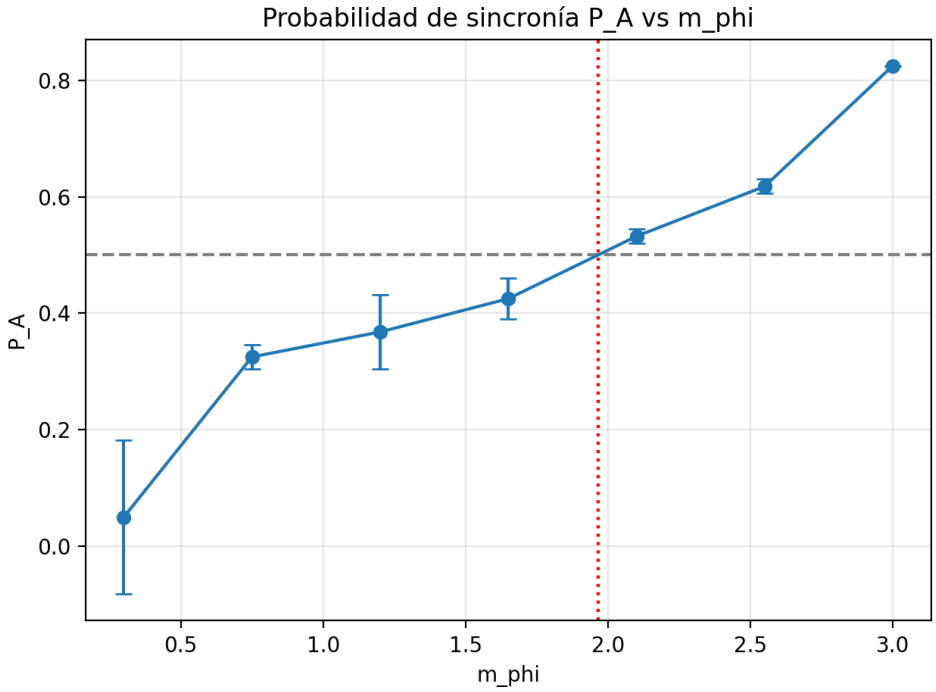

Figure 1: Synchrony probability $P_A(m_\phi)$ averaged over k_{rot}. Dashed line: $P_A = 0.5$. Dotted vertical: $m_{\phi,\text{crit}} \simeq 1.965$.

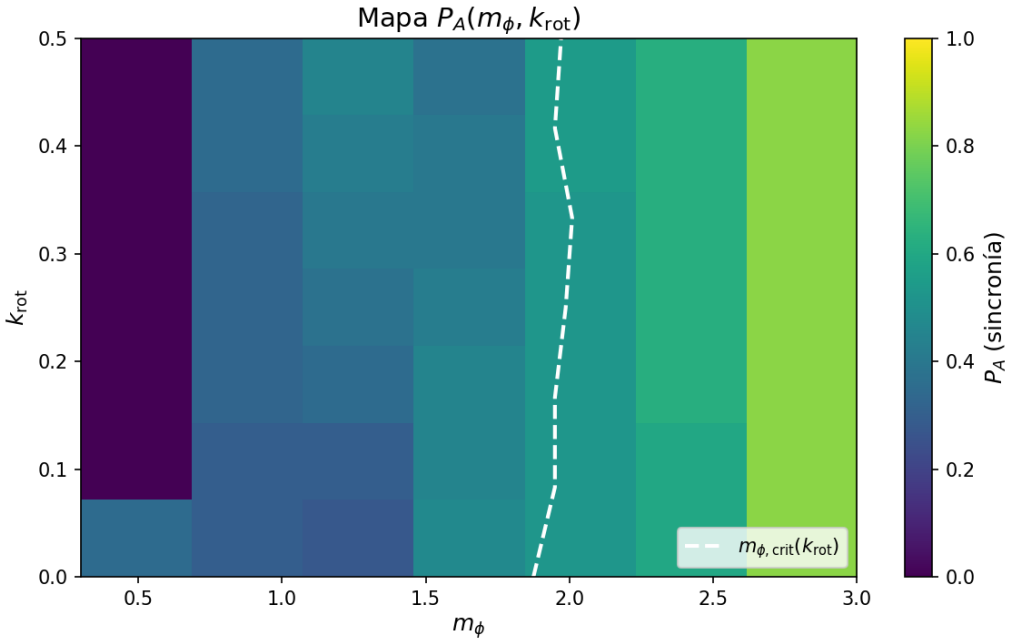

Figure 2: 2D map $P_A(m_\phi, k_{\text{rot}})$. White dashed: locus $P_A = 0.5$ i.e. local $m_{\phi,\text{crit}}(k_{\text{rot}})$. Nearly vertical transition band.

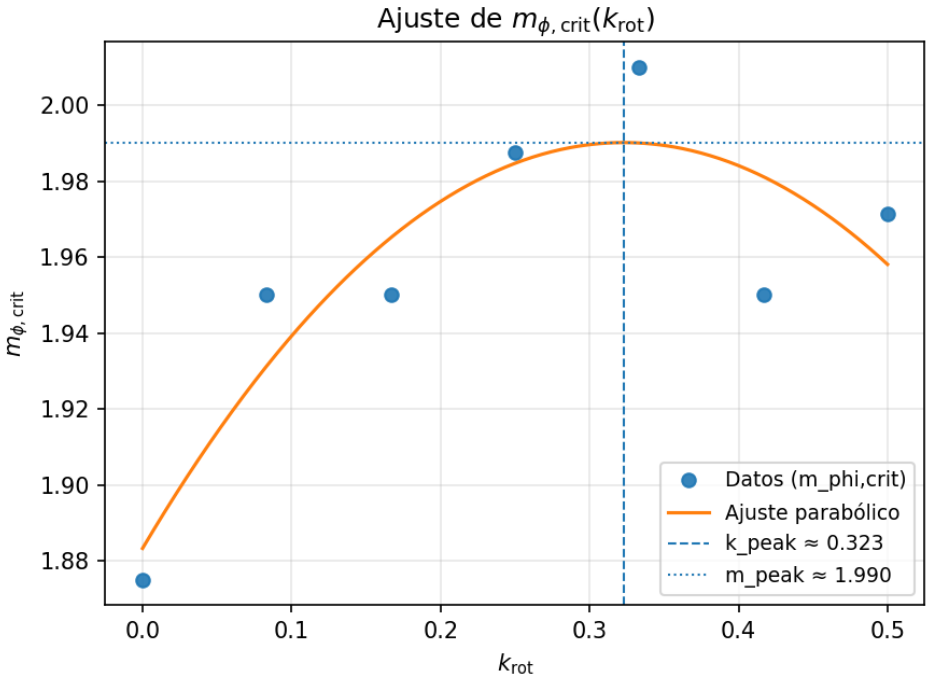

Figure 3: Quadratic fit to $m_{\phi,\mathrm{crit}}(k_{\mathrm{rot}})$ showing a weak maximum near $k_{\mathrm{rot}} \simeq 0.33$.

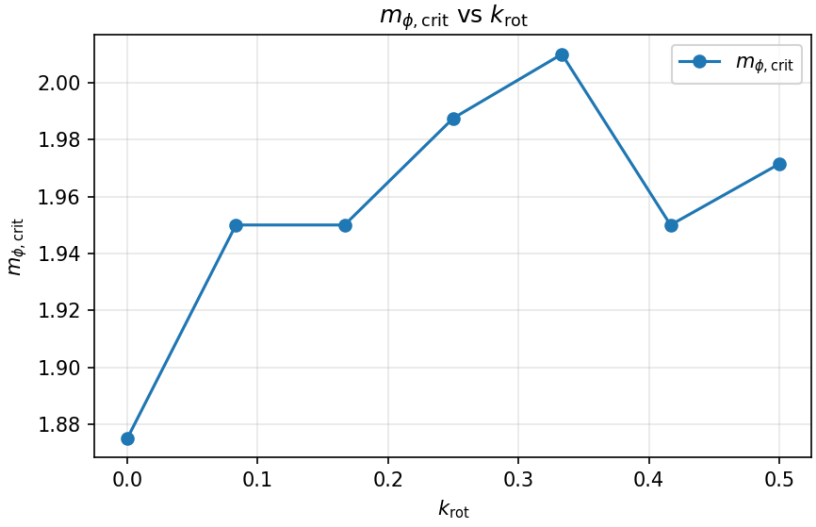

Figure 4: Discrete points used in the fit of Fig. 3.

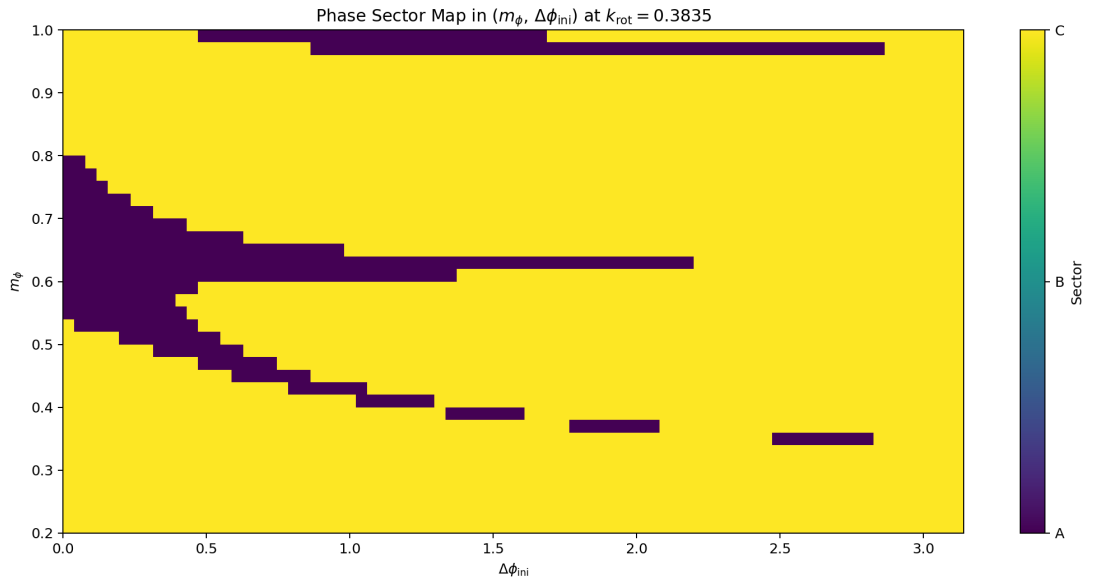

Figure 5: Phase-sector map in $(m_\phi, \Delta\phi_{\text{ini}})$ at representative k_{rot}. Dark: synchrony (A). Yellow: escape (C).

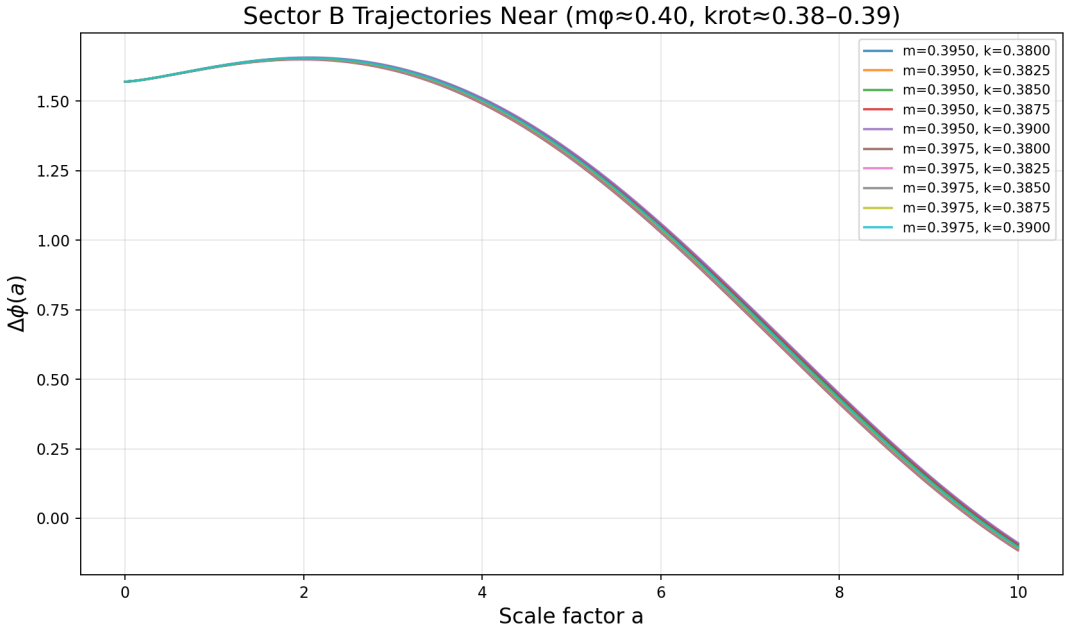

Figure 6: Representative trajectories in sector B (antipodal trapping) near ($m_\phi \simeq 0.40$, $k_{\text{rot}} \simeq 0.38$–$0.39$).

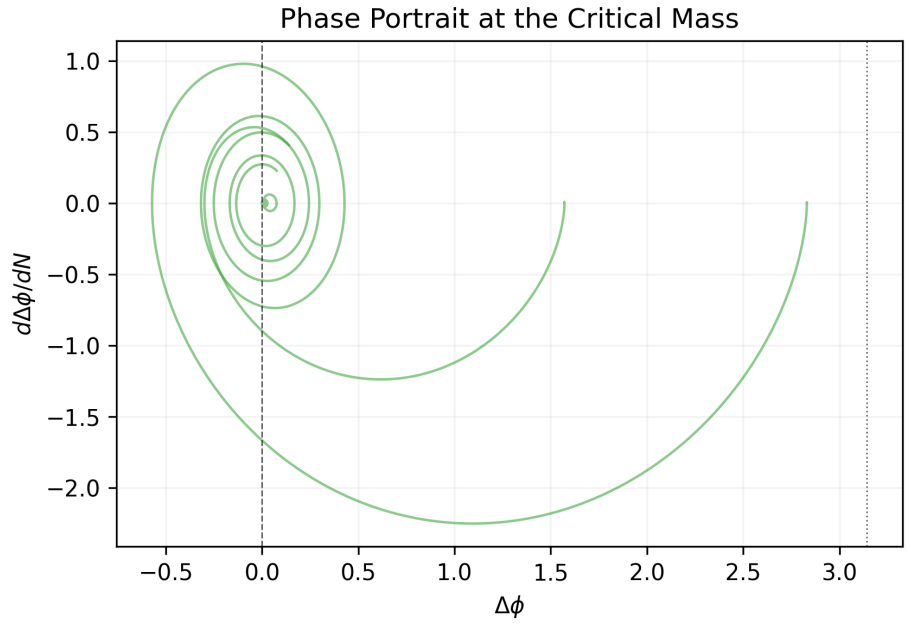

Figure 7: Phase portrait at $m_{\phi,\mathrm{crit}}$: estable espiral en $\Delta\phi = 0$ y separatriz suave.

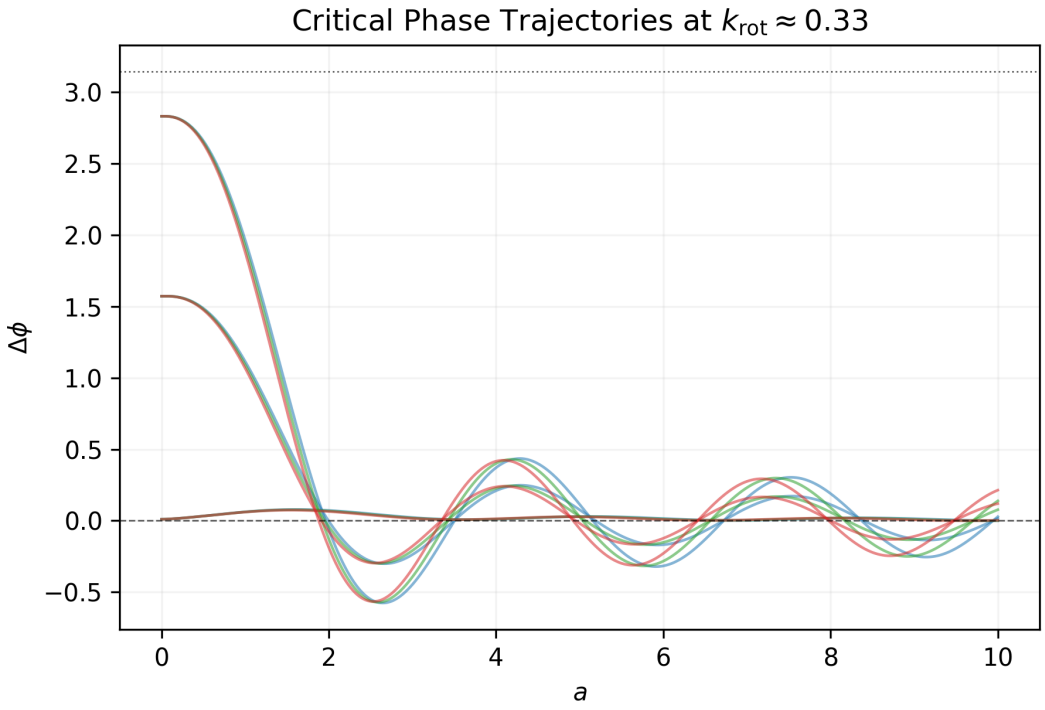

Figure 8: Near-critical families of trajectories around $k_{\mathrm{rot}} \simeq 0.33$ ilustrando el origen del salto suave en $P_A(m_\phi)$.

5 Data & Reproducibility

All figures are generated from artefacts in `results_phase_sectors/`. **Figures (PNG):** `PA_vs_mphi.png`, `PA_map_mphi_krot_with_mcrit.png`, `mphi_crit_vs_krot_fit.png`, `mphi_crit_vs_krot.png`, `phase_sector_map_delta.png`, `sectorB_trajectories.png`, `crit_phase_portrait.png`, `crit_trajectorie`
Grid: m_ϕ and $k_{\rm rot}$ values as above; $N_\Delta = 40$; $\Delta\phi_{\rm ini} \sim \mathcal{U}[0, \pi)$. **Integrator:** RK45 with `rtol`$= 10^{-7}$, `atol`$= 10^{-9}$; $\Delta N_{\max} = 10^{-2}$. **Window:** $N_{\rm ini} = -4$, $N_f = +10$; late averages on $\Delta N = 1$. **Thresholds:** $\epsilon_\phi = 0.1$, $\epsilon_\pi = 0.1$, $\epsilon_{\phi'} = 0.05$. **Seed:** 42.
Post-processing: (i) $P_A = N_A/N_\Delta$; (ii) interpolate $P_A(m_\phi)$ to $P_A = 0.5$; (iii) compute $m_{\phi,\rm crit}(k_{\rm rot})$ and fit $ak_{\rm rot}^2 + bk_{\rm rot} + c$.

6 Discussion and Outlook

Our grid scan confirms a smooth transition yielding a well-defined $m_{\phi,\rm crit}$. The near-vertical band in $(m_\phi, k_{\rm rot})$ and the modest peak of $m_{\phi,\rm crit}(k_{\rm rot})$ around 0.33 indicate that rotation slightly shifts the separatrix but does not alter the basic fate map. The portrait at $m_{\phi,\rm crit}$ exhibits a single stable spiral at $\Delta\phi = 0$, consistent with a damped nonlinear oscillator. Next steps include embedding the dynamics in a calibrated ΛCDM background and replacing the uniform prior on $\Delta\phi_{\rm ini}$ by a quantum-motivated distribution; on the observational side, FRB and CMB anisotropies provide falsifiable tests.

Acknowledgements

We thank the open-science community for tools enabling this analysis. We acknowledge Grok (xAI) for critical feedback and ChatGPT (Toko) for assistance in structuring, documenting and validating the workflow.

References

References

[1] L. Boyle, K. Finn and N. Turok, CPT-Symmetric Universe, *Phys. Rev. Lett.* **121**, 251301 (2018).

[2] R. Lasenby, M. D. Schwarz and J. D. Barrow, CPT symmetry in cosmology and the Archaic Universe, *Phys. Scripta* **95**, 075004 (2020).

[3] J.-P. Petit, CPT Symmetry in Two-Fold de Sitter Universe, *Symmetry* **13**, 375 (2021).

[4] J.-P. Petit and G. d'Agostini, A bimetric cosmological model based on Andreï Sakharov's twin-universe, *Eur. Phys. J. C* **84**, 1123 (2024).

[5] D. J. E. Marsh, Axion Cosmology, *Phys. Rept.* **643**, 1–79 (2016).

[6] Y. Kuramoto, *Chemical Oscillations, Waves, and Turbulence*, Springer (1984).

[7] S. H. Strogatz, From Kuramoto to Crawford: Exploring the onset of synchronization in populations of coupled oscillators, *Physica D* **143**, 1–20 (2000).

[8] CosmicThinker & ChatGPT (Toko), *Phase-Bifurcation Cosmogenesis v3.0 Repro Pack*, Zenodo (2025). DOI: `to-be-assigned`.

[9] CosmicThinker & ChatGPT (Toko), *mphi_crit Grid Scan & Figures (results_phase_sectors/)*, Zenodo (2025). DOI: `to-be-assigned`.